Reprod Fertil Dev. Author manuscript; available in PMC 2010 June 08.

Published in final edited form as:

Reprod Fertil Dev. 2009 ; 21(4): 579–586. doi:10.1071/RD08295.

Ovarian imaging in the mouse using ultrasound biomicroscopy (UBM): a validation study

Carmen N. Mircea[A], **Marla E. Lujan**[A], **Rajesh S. Jaiswal**[B], **Jaswant Singh**[B], **Gregg P. Adams**[B], and **Roger A. Pierson**[A,C]

[A] Obstetrics, Gynecology and Reproductive Sciences, College of Medicine, University of Saskatchewan, Saskatoon, Saskatchewan, S7N 0W8, Canada

[B] Veterinary Biomedical Sciences, Western College of Veterinary Medicine, University of Saskatchewan, Saskatoon, Saskatchewan, S7N 5B4, Canada

Abstract

The mouse is a well accepted model for studies of human reproduction despite little being known about follicle dynamics in this species. Longitudinal studies of mouse folliculogenesis have been hampered by the lack of an appropriate imaging tool. Ultrasound biomicroscopy (UBM) may overcome this obstacle as it confers near-microscopic resolution through the use of high-frequency ultrasound waves. The objective of the present study was to determine whether UBM could be used to count and measure ovarian follicles and corpora lutea (CL) reliably in mice. Ovaries of 25 adult CD-1 mice were imaged using a 55-MHz transducer and then excised and processed for histology. Follicles and CL were counted and measured from digitally stored UBM cine-loops and photographed histological sections. Differences between techniques were assessed by Bland-Altman agreement analyses. Follicle counts yielded by the two techniques varied by only ±1 follicle when follicles ranged between 300 and 499 μm. Perfect agreement among counts was evident when follicles were >500 μm. The total number of CL was accurately estimated using UBM; however, the number of 350–699 μm CL was underestimated and the number of CL ≥700 μm was overestimated. In conclusion, UBM can be used reliably to count and measure follicles in mice.

Additional keywords

corpora lutea; histology; ovarian follicles; ultrasonography

Introduction

The mouse is widely used as a mammalian model for studies in reproductive biology. Mice are easy to handle, require little maintenance, are widely available and have a short oestrous cycle. Although we commonly translate findings from research of the reproductive system made in mice to humans, it should be acknowledged that we know very little about the characteristics of ovarian follicle dynamics in mice. To date, patterns of follicle and corpus

[C]Corresponding author. pierson@erato.usask.ca.

luteum (CL) development during the oestrous cycle have been inferred from histologic and endocrine assessments (Long and Evans 1922; Mandl and Zuckerman 1952; Hirshfield and Midgley 1978; Numazawa and Kawashima 1982; Hirshfield 1987; Gaytán *et al.* 1997). Since histology captures only a single instance in the physiology of a particular animal, this limitation has hindered our understanding of dynamic processes such as folliculogenesis. We are unaware of any published data describing a longitudinal, *in vivo* evaluation of follicle and CL dynamics during a natural murine reproductive cycle. This is in contrast to other species, such as horses, cattle and humans, in which detailed serial ultrasonography and endocrine measurements have been used to characterise follicle growth and regression, ovulation and luteal function (Pierson and Ginther 1984, 1985*a*, 1985*b*, 1987; Quirk *et al.* 1986; Baerwald *et al.* 2003, 2005).

Our knowledge of murine follicular dynamics has been limited by the lack of a non-invasive imaging tool that could be used for the serial assessment of ovarian structures in small laboratory animals. In the 1980s, development of real-time ultrasonography using 5- to 7.5-MHz transducers allowed for reliable imaging of the reproductive tracts of large domestic animals, such as mares and heifers (Pierson and Ginther 1984, 1985*a*, 1985*b*, 1987). Acoustic beams in this frequency range provided fair resolution of structures as small as 2–3 mm and serial imaging using a transrectal approach led to the first description of the kinetics of follicle development, ovulation and luteal function in these species (Pierson and Ginther 1984, 1985*a*, 1985*b*, 1987). The development of higher frequency transducers in the 1990s, coupled with advances in computer technology, allowed for far better resolution of ovarian structures than previously possible.

Ultrasound biomicroscopy (UBM) allows for near-microscopic, high-resolution *in vivo* imaging of organ systems in small laboratory animals, such as mice and rats, by employing ultra-high frequency ultrasound waves (30–55 MHz) (Turnbull *et al.* 1995; Foster *et al.* 2000, 2002; Coatney 2001; Zhou *et al.* 2002). The eye, skin, heart, kidney, cartilage, tumour masses and embryos of rats and mice have been imaged in earlier studies (Turnbull *et al.* 1995; Foster *et al.* 2000, 2002; Coatney 2001; Zhou *et al.* 2002; Pallares *et al.* 2009) and a recent study suggests it may even be possible to image small antral follicles in the rat ovary (Pallares and Gonzalez-Bulnes 2008). Ultra-high frequency sound waves in the 30–50 MHz range have dramatically improved spatial resolution; however, the major limitation of this technology is that beam attenuation is increased and tissue penetration decreased. Since mouse ovaries are situated close to the dorsal body wall and mice have thin tissue layers, the limited penetration of UBM may not be a significant impediment to *in vivo* imaging. A recent report by Pallares *et al.* documenting good visualisation of ovarian structures in cycling mice and following ovarian stimulation would suggest that this is the case (Pallares and Gonzalez-Bulnes 2008). The near-microscopic resolution provided by UBM may mark the beginning of many new approaches to the study of female reproductive physiology if we can validate this method for measuring and identifying patterns in follicle development, ovulation and regression.

The objective of the present study was to determine whether UBM technology could be used to count and measure follicles and CL reliably in the mouse ovary *in vivo*. We defined reliability as the ability to obtain similar counts and measurements on UBM and histology.

We hypothesised that UBM technology could be used reliably to quantify follicle and CL development in mouse ovaries *in vivo*.

Materials and methods

Animals

Adult female CD-1 mice, ranging from 5 to 12 weeks of age and weighing ~30 g were housed in proximity to adult male CD-1 mice. Food and water were available *ad libitum*. The housing environment followed a photoperiod schedule of 14 h of light and 10 h of darkness (lights on at 0700 hours). An ambient temperature of 21°C was maintained. The females were individually identified and their vaginal smears were examined and recorded daily over a two-cycle acclimatisation period. Female mice exhibiting consecutive, regular oestrous cycles of a 5-day duration ($n = 25$) were selected for the study. Animals were scanned and killed at various stages of the oestrous cycle. All experimental procedures conformed to the International Guiding Principles for Biomedical Research Involving Animals and were approved by the Animal Care Committee of the University of Saskatchewan (Saskatoon, SK, Canada).

Ultrasound biomicroscope

The ultrasound biomicroscope (Vevo 660, Visual Sonics, Toronto, ON, Canada) is a high-resolution acoustic imaging system consisting of a mechanical scanhead and associated signal and image processing hardware. A computer running Windows NT was used to control system timing, motion control, scan conversion and display. The ultrasound biomicroscope operated over a frequency range of 30–70 MHz. Prior to commencing the present study, a trial was performed to determine the machine settings that provided optimal visualisation of the ovaries. The following machine settings were found best suited for obtaining ovarian images in mice when both image resolution and necessary depth of penetration were considered: transducer with a 55-MHz central frequency (Real-time Micro-Visualisation, RMV 708), power 79%, radio frequency 1 kHz, master gain −1 dB, delay 0.48 mm, field of view 6.49 mm × 6.49 mm, frame rate 30 Hz, range 12 dB. At 55 MHz centre frequency, the lateral resolution of linear beams was 60 μm and the maximum imaging depth was ~6.5 mm. The fixed focal point was 4.5 mm from the transducer surface.

Ovarian imaging technique

Each mouse was initially placed in a 3% isofluorane anaesthesia apparatus. Once anesthetised, the mouse was transferred onto a platform with X and Y movement controls, positioned in sternal recumbency and maintained on continuous 1.5% isofluorane. The dorsolateral body hair coat was removed with hair removal cream (NAIR, Church and Dwight Canada Corp., Missassagua, ON, Canada) and ultrasound contact gel (Eco Gel 200, Eco-Med Pharmaceutical Inc., Mississauga, ON, Canada) was applied to the hair-free aspect of the back in the lumbar region. The transducer, which was fixed onto a custom-designed holder from above, was then gently lowered into contact with the surface of the skin. The transducer was first positioned on the right dorsolateral side of the mouse. The platform was then moved cranially to caudally until the right ovary was visualised. Kidneys were used as a landmark as they are situated cranially to ovaries. Once the ovary was identified, the

platform was steered slowly from medial to lateral aspects of the ovary and images were recorded digitally (300 frames per 10-s cine-loop). The transducer was then transferred onto the left dorsolateral side of the mouse and the same procedure was followed to image the left ovary.

Ovarian collection and histology

Following imaging, the mice were killed by an overdose of isofluorane. A mid-ventral incision was made and the abdominal contents dissected to expose the ovaries. Ovaries were removed, cleaned of debris and fat, placed in labelled processing cassettes, fixed in 10% neutral-buffered formalin and stored at room temperature until histological processing. Fifty ovaries from mice at various stages of the oestrous cycle, and in pregnant and pseudopregnant states were sectioned at a 70-μm thickness with a cryotome (CM3050S; Leica Microsystems, Nussloch, Germany). Serial sections were collected and placed on poly-L-lysine-coated slides. Sections were stained with hematoxylin and eosin and mounted using non-water-miscible mounting media. Slides were examined with a light microscope system (Carl Zeiss, Jena, Germany) using the 2.5× objective lens and digital pictures of the sections were captured (Sony Cyber-shot DSC-V3; Sony of Canada Ltd, Toronto, ON, Canada).

Our objective was to count antral follicles larger than 150 μm accurately and not to assess the status (healthy, regressing, advanced atretic). Therefore, we used serial sections of the ovary at this unusual thickness which allowed us to count every antral follicle after aligning adjoining serial slices. This reduced the labour substantially. We could determine the position of very large follicles and corpora lutea from adjacent sections to avoid double counting.

Counting and measuring of follicles and corpora lutea

Two custom-developed software programs (FRAME and SYNERGYNE 2, Synergyne Inc., Saskatoon, SK, Canada) were used to analyse the digital UBM cine-loops. Recordings could be viewed at any speed or direction including frame-by-frame analysis. Colour and contrast adjustments and linear measurements could be made on any frame of the video clip. For each of the fifty UBM cine-loops (one digital recording for each ovary), individual follicles and corpora lutea were identified, counted and measured by scrolling through the digital recordings frame-by-frame. The frame containing the largest cross-sectional area of the follicle or CL in question was selected and the largest and widest orthogonal diameters were measured. The size (μm) reported for each of the follicles and CL was derived from the mean of the two diameter measurements.

Digital images of the histological sections for each ovary were sequentially loaded onto the Image J NIH Software System (National Institutes of Health, Bethesda, MD, USA). For each ovary, ~38 histological sections and digital images were generated. For each of the fifty ovaries, individual follicles and corpora lutea were identified, counted and measured by scrolling through the serial digital images. A protocol similar to that used to assess UBM images was used to count and measure follicles and CL. All ultrasonographic and histological measurements and counts were performed by a single observer.

Statistical analysis

The level of agreement in total follicle and CL counts yielded by UBM and histology was assessed by Bland-Altman agreement analysis. To determine if counts were consistent among different-sized follicles and CL, Bland-Altman agreement analyses were performed on counts stratified by size (follicle size: 200–299 μm, 300–399 μm, 400–499 μm and ≥500 μm; CL size: <350 μm, 350–699 μm and ≥700 μm). The Bland-Altman agreement analysis measured the degree to which the new technique (i.e. UBM) estimated the gold standard (i.e. histology). This approach involved tabulating the average difference between counts – called the *bias* – and their corresponding standard deviations (Bland and Altman 1986). Therefore, the bias represented the average number of counts under- or overestimated by UBM compared with histology while the limits of agreement represented the range at which follicles or CL were missed or over-counted using UBM. Acceptable deviation from measurements obtained from the gold standard is a decision based on clinical relevance.

Results

Follicles

Follicles at different stages of development were clearly evident in images of mouse ovary taken by UBM and histology (Fig. 1). Antral follicles appeared as spherical anechoic structures (arrows) scattered among stromal and luteal tissue on UBM (Panel *a*). We were able to distinguish small antral follicles ranging in size from 300 to 450 μm in a single ovary as well as larger preovulatory follicles measuring greater than 700 μm (Panel *b*). A histological section through the ovary in Panel *a* confirmed the presence of multiple follicles at similar stages of development (Panel *c*).

The average number of follicles counted per ovary using UBM and histology are presented in Table 1 and the corresponding bias plots generated by the Bland-Altman agreement analyses are shown in Fig. 2. The total number of follicles estimated by UBM was slightly lower than the total number of follicles counted by histology (differed by four follicles). Stratification of counts by follicle size showed that counts made by UBM underestimated the number of follicles sized between 200 and 299 μm, but estimated the number of follicles larger than 300 μm reliably (counts varied by only ±1 follicle).

Corpora lutea

Corpora lutea were also evident in images of mouse ovary taken by UBM and histology (Fig. 3). Corpora lutea appeared as variable-sized areas of heterogeneous echotexture scattered among less concentrated, but more pronounced, hyperechoic stromal tissue and anechoic follicles (arrows). The right half of the ovary in Panel *a* depicts two seemingly large CL (780 and 970 μm) on either side of a 287-μm follicle. For ease of image interpretation, luteal structures are outlined in Panel *b*. Upon histologic examination, it was apparent that CL typically ranged in size from 200 to 750 μm and were generally not larger than 750 μm. The histological section in Panel *c* demonstrates the presence of CL ranging from 270 to 570 μm. Distinct fine margins among adjacent CL were evident on histology (arrows) but not on UBM.

The average number of CL counted per ovary using UBM and histology are presented in Table 2 and the corresponding bias plots generated by the Bland-Altman agreement analyses are shown in Fig. 4. The total number of CL estimated by UBM was slightly lower than that counted by histology (differed by only four CL). Stratification by CL size showed that UBM could be used to estimate the number of CL smaller than 350 μm reliably. In contrast, counts made by UBM underestimated the number of CL between 350 and 699 μm (by ~12 CL) and overestimated the number of CL that appeared to be >700 μm (by ~8 CL).

Discussion

The hypothesis that UBM could be used reliably to quantify follicle and CL development in mouse ovaries *in vivo* was supported. Comparison of follicle counts made on UBM scans and histological sections showed good agreement in estimating the total number of follicles >300 μm in each ovary. While UBM was recently shown to provide outstanding images of both follicles and CL in cycling and non-cycling mice and rats (Pallares and Gonzalez-Bulnes 2008), we extend these observations by showing that UBM could be used reliably to discriminate follicles that differed in size by 100 μm and to identify all preovulatory-sized follicles in the fifty ovaries studied (up to 1093 μm). Luteal tissue within the mouse ovary was readily distinguished from stroma and follicles. However, the good agreement reported among total CL counts was futile as the dimensions of individual CL could not be consistently measured using UBM.

The ability to distinguish follicles with diameters ranging from 300 to >500 μm with UBM is an important finding since follicle selection in rodents is theorised to occur at ~350 to 400 μm and ovulation occurs when follicles are >400 μm (Hirshfield and Midgley 1978; Numazawa and Kawashima 1982; Rose *et al.* 1999). There was near-perfect agreement between UBM and histology counts within these follicle dimensions, supporting the notion that UBM may be used to assess the transition to selection and ovulation in the murine model. Although UBM has been reported to achieve resolution as small as 60 μm (Foster *et al.* 2002), varying amounts of subcutaneous fat tissue among animals sometimes interfered with optimal visualisation of ovarian follicles. However, we do not suspect that difficulty in visualising follicles smaller than 300 μm will hamper future endeavours designed to elucidate follicle dynamics in mice. Growth rates for this follicle size category are described as constant suggesting a continuous turnover of small follicles during the oestrous cycle (Mandl and Zuckerman 1952; Hirshfield and Midgley 1978).

The number of CL visualised by either histology or UBM was substantially higher than the number of follicles reported. This observation was consistent with a previous morphometric study of the mouse ovary (Numazawa and Kawashima 1982). A previous histological study estimated the total number of CL in a pair of mouse ovaries at ~40 at proestrus with 10 new CL forming at each oestrus (Numazawa and Kawashima 1982). Considering that four cycles are necessary for luteolysis, mouse ovaries would be expected to be rich in luteal tissue at different stages of development or regression at any point in time (Numazawa and Kawashima 1982). Newly formed CL are typically 400 to 600 μm in diameter after ovulation and 350 to 700 μm at metestrus (Numazawa and Kawashima 1982). We classified CL in three size groups with the assumption that CL measuring <350 μm would represent a

regressing CL pool, while those 350–699 μm would represent newly formed CL. The addition of a ≥700 μm size category was based on our initial evaluation of the UBM images, which showed a prevalence of larger CL.

Agreement for CL counts made by UBM and histology was variable for the different size categories. Good agreement was found for CL smaller than 350 μm. However, very few CL measuring <350 μm were present on either UBM or histology (ranging from 0 to 5 CL per ovary). Although we could distinguish luteal tissue from follicles and stroma reliably using UBM, good agreement among overall counts was somewhat misleading since it actually represented an undercounting of CL 350 to 699 μm and an overcounting of CL ≥700 μm. Histological assessment confirmed that most CL ranged from 350 to 699 μm (14 to 41 per ovary) and few CL were actually ≥700 μm (0 to 2 per ovary). The overestimation of CL ≥700 μm was attributed to difficulty in distinguishing interfaces between adjacent CL on UBM. It was evident upon assessment of the histological sections that several luteal structures that appeared to be >1000 μm on UBM were actually two or three closely apposed individual CL. The difficulty in resolving adjacent luteal structures may be overcome when serial ultrasonography is employed to generate a dynamic image profile of CL over several oestrous cycles. However, we cannot exclude the possibility that detection of large CL on UBM, but not on histology, was the result of tissue shrinkage following fixation and tissue processing.

It is important to acknowledge that there are limitations inherent to ultrasonographic-histomorphometric assessments and a certain lack of agreement between UBM and histologic measurements was inevitable. Follicles and CL were stratified by group sizes by averaging the longest and widest orthogonal diameters. The structures were identified and measured on successive 70-μm histology sections and ultrasound frames that approximated 10-μm slices. The probability that the ultrasound frames and histology sections contained the longest and widest diameters for the same plane was low. In general, follicles and CL tended to be undercounted when using UBM. However, we considered the difference between counts (or the bias) to fall within an acceptable range. On average, only 14% of CL and only 28% of follicles – all of which were <300 μm – were missed and they are part of what has been described as a constant follicle pool (Mandl and Zuckerman 1952; Hirshfield and Midgley 1978).

One of the major limitations of UBM encountered during the present study was related to the decreased depth of penetration of the high-frequency transducer. Poorer visualisation of the deeper segments of the ovaries was common in heavier mice that had more subcutaneous fat tissue. In the present study, UBM settings were held constant when imaging all 25 mice. There was potential to alter frequency, depth of penetration, focal length, and other image controls for each scan; however, we elected not to alter settings for each animal since we anticipated subjecting the images to detailed computer analysis. The UBM technology is promising once improved penetration of ultrasound beam and better image resolution are available. Imaging advances could potentially eliminate difficulty in distinguishing interfaces between adjacent CL and imaging ovaries of heavier animals.

There is tremendous variability in the response to standard ovarian stimulation protocols for assisted reproduction, ovarian suppression for hormonal contraception and the natural transition to ovarian senescence in women. Improving small animal models for studies to elucidate human reproductive biology is a critical part of enhancing our understanding of these phenomena. Although serial ultrasonography can be used in women and in larger, well accepted animal models to study human ovarian function (Pierson and Ginther 1984, 1985*a*, 1985*b*, 1987; Baerwald *et al.* 2003, 2005), small laboratory animals have the advantage of being more accessible, easier to handle and less expensive to maintain. Additionally, the experiments involving small animal models are of short duration due to the shorter length of the oestrous cycle and pregnancy. These advantages facilitate the faster development and testing of new pharmaceutical interventions and allow for economically feasible means of determining possible long-term adverse effects of these interventions. Application of serial *in vivo* imaging technology in small animals also has important implications in furthering our commitment to reduce the number of laboratory animals used in scientific studies. Moreover, UBM technology will improve the validity of prospective studies aimed at evaluating ovarian function, as effects in individual animals can be followed for the duration of a study.

Conclusion

In conclusion, we have demonstrated that antral follicles in mouse ovaries could be reliably counted and measured using UBM. Luteal tissue could be reliably distinguished from ovarian follicles and stroma in the mouse although interfaces between adjacent CL were often difficult to resolve and gave the semblance of larger luteal structures within the ovary. UBM promises to be an excellent tool to elucidate follicle dynamics in mice and, therefore, may represent the long-awaited tool that provides us with a fully validated small animal model for studies of human reproduction.

Acknowledgments

This work was supported by grants from the Natural Sciences and Engineering Research Council of Canada (NSERC) and the Canadian Institutes of Health Research (CIHR, MOP 11489), and resources of the Reproductive Science and Medicine Research Group, University of Saskatchewan. C.N.M. and M.E.L. were supported by Strategic Training Initiative in Research in the Reproductive Health Sciences (STIRRHS) scholarships awarded by the Association of Professors of Obstetrics and Gynaecology of Canada (APOG) and CIHR.

References

Baerwald AR, Adams GP, Pierson RA. Characterisation of ovarian follicular wave dynamics in women. Biol Reprod. 2003; 69:1023–1031. DOI: 10.1095/BIOLREPROD.103.017772 [PubMed: 12748128]

Baerwald AR, Adams GP, Pierson RA. Form and function of the corpus luteum during the human menstrual cycle. Ultrasound Obstet Gynecol. 2005; 25:498–507. DOI: 10.1002/UOG.1891 [PubMed: 15846762]

Bland JM, Altman DG. Statistical methods for assessing agreement between two methods of clinical measurement. Lancet. 1986; 1:307–310. [PubMed: 2868172]

Coatney RW. Ultrasound imaging: principles and applications in rodent research. ILAR J. 2001; 42:233–247. [PubMed: 11406722]

Foster FS, Pavlin CJ, Harasiewicz KA, Christopher DA, Turnbull DH. Advances in ultrasound biomicroscopy. Ultrasound Med Biol. 2000; 26:1–27. DOI: 10.1016/S0301-5629(99)00096-4 [PubMed: 10687788]

Foster FS, Zhang MY, Zhou YQ, Liu G, Mehi J, et al. A new ultrasound instrument for *in vivo* microimaging of mice. Ultrasound Med Biol. 2002; 28:1165–1172. DOI: 10.1016/S0301-5629(02)00567-7 [PubMed: 12401387]

Gaytán F, Bellido C, Morales C, Aguilar E, Sanchez-Criado JE. Follicular growth pattern in cyclic rats from late pro-oestrus to early oestrus. J Reprod Fertil. 1997; 110:153–159. DOI: 10.1530/JRF.0.1100153 [PubMed: 9227369]

Hirshfield AN. Histological assessment of follicular development and its applicability to risk assessment. Reprod Toxicol. 1987; 1:71–79. DOI: 10.1016/0890-6238(87)90074-8 [PubMed: 2980367]

Hirshfield AN, Midgley AR Jr. Morphometric analysis of follicular development in the rat. Biol Reprod. 1978; 19:597–605. DOI: 10.1095/BIOLREPROD19.3.597 [PubMed: 363183]

Long, JA., Evans, HM. Memoirs of the University of California Press. University of California Press; Berkeley, CA: 1922. The oestrous cycle of the rat and its associated phenomena.

Mandl AM, Zuckerman S. Cyclical changes in the number of medium and large follicles in the adult rat ovary. J Endocrinol. 1952; 8:341–346. DOI: 10.1677/JOE.0.0080341 [PubMed: 12990735]

Numazawa A, Kawashima S. Morphometric studies on ovarian follicles and corpora lutea during the oestrous cycle in the mouse. J Reprod Fertil. 1982; 64:275–283. DOI: 10.1530/JRF.0.0640275 [PubMed: 7200138]

Pallares P, Gonzalez-Bulnes A. The feasibility of ultrasound biomicroscopy for non-invasive and sequential assessment of ovarian features in rodents. Reprod Biol. 2008; 8:279–284. [PubMed: 19092988]

Pallares P, Fernandez-Valle ME, Gonzalez-Bulnes A. *In vivo* virtual histology of mouse embryogenesis by ultrasound biomicroscopy and magnetic resonance imaging. Reprod Fertil Dev. 2009; 21:283–292. DOI: 10.1071/RD08124 [PubMed: 19210919]

Pierson RA, Ginther OJ. Ultrasonography of the bovine ovary. Theriogenology. 1984; 21:495–504. DOI: 10.1016/0093-691X(84)90411-4 [PubMed: 16725899]

Pierson RA, Ginther OJ. Ultrasonic evaluation of the corpus luteum of the mare. Theriogenology. 1985a; 23:795–806. DOI: 10.1016/0093-691X(85)90155-4 [PubMed: 16726050]

Pierson RA, Ginther OJ. Ultrasonic evaluation of the preovulatory follicle in the mare. Theriogenology. 1985b; 24:359–368. DOI: 10.1016/0093-691X(85)90228-6 [PubMed: 16726090]

Pierson RA, Ginther OJ. Ultrasonographic appearance of the bovine uterus during the oestrous cycle. J Am Vet Med Assoc. 1987; 190:995–1001. [PubMed: 3570959]

Quirk SM, Hickey GJ, Fortune JE. Growth and regression of ovarian follicles during the follicular phase of the oestrous cycle in heifers undergoing spontaneous and PGF-2-alpha-induced luteolysis. J Reprod Fertil. 1986; 77:211–219. DOI: 10.1530/JRF.0.0770211 [PubMed: 3522890]

Rose UM, Hanssen RG, Kloosterboer HJ. Development and characterisation of an *in vitro* ovulation model using mouse ovarian follicles. Biol Reprod. 1999; 61:503–511. DOI: 10.1095/BIOLREPROD61.2.503 [PubMed: 10411533]

Turnbull DH, Bloomfield TS, Baldwin HS, Foster FS, Joyner AL. Ultrasound backscatter microscope analysis of early mouse embryonic brain development. Proc Natl Acad Sci USA. 1995; 92:2239–2243. DOI: 10.1073/PNAS.92.6.2239 [PubMed: 7892254]

Zhou YQ, Foster FS, Qu DW, Zhang M, Harasiewicz KA, Adamson SL. Applications for multifrequency ultrasound biomicroscopy in mice from implantation to adulthood. Physiol Genomics. 2002; 10:113–126. [PubMed: 12181368]

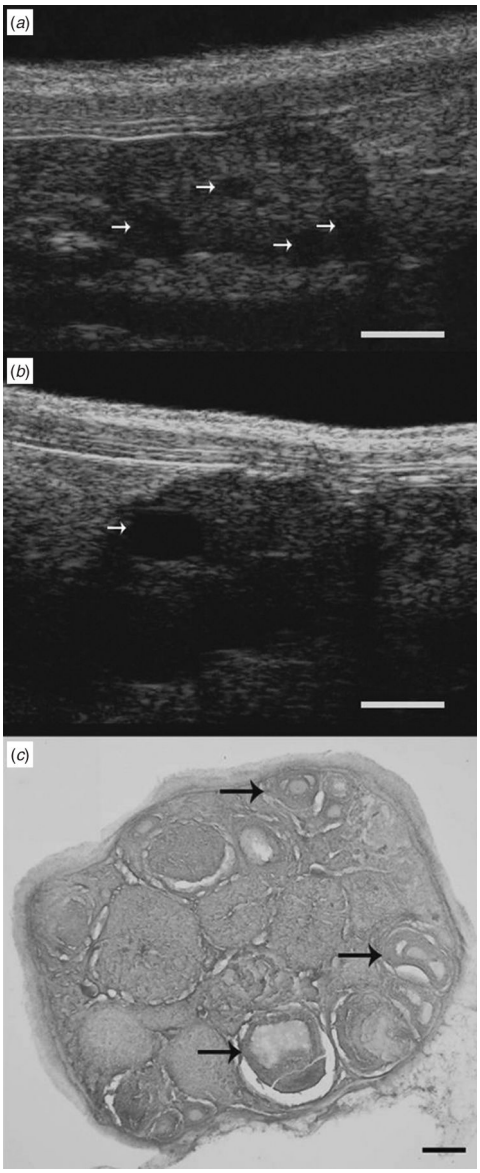

Fig. 1.

Ultrasound biomicroscopy and histological sections of a mouse ovary depicting follicles at different stages of development. Arrows on UBM images indicate ovarian follicles ranging from (*a*) 290 to 440 μm in diameter and (*b*) a preovulatory-sized follicle measuring 730 μm in diameter. (*c*) The arrows in the histological image indicate ovarian follicles ranging from 220 to 385 μm in diameter. Scale bar: (*a*, *b*) 1000 μm, (*c*) 200 μm.

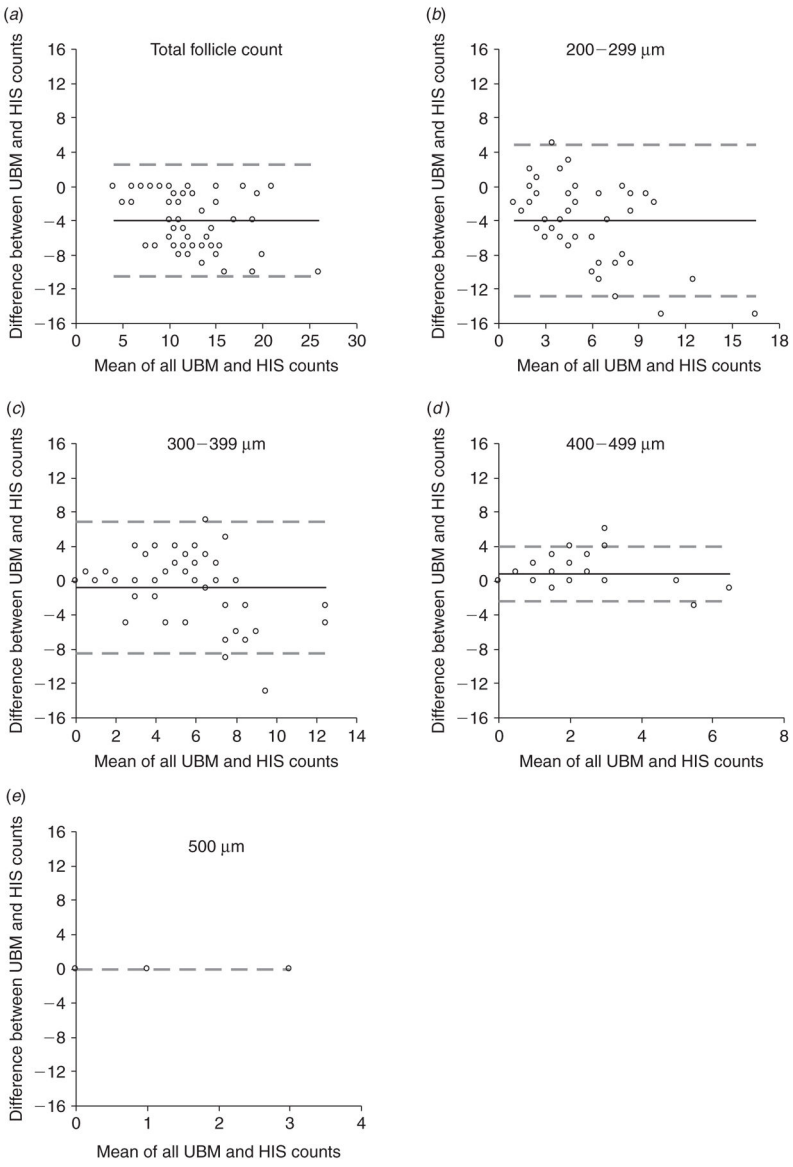

Fig. 2.

Bland-Altman plots for differences in counts made by ultrasound biomicroscopy (UBM) and histology (HIS) for (*a*) the total number of follicles, (*b*) follicles 200–299 μm in diameter, (*c*) follicles 300–399 μm in diameter, (*d*) follicles 400–499 μm in diameter and (*e*) follicles ≥500 μm in diameter. Ovarian follicles <300 μm were undercounted by UBM, whereas counts were in agreement when follicles were >300 μm. Bias is represented by a solid line. Limits of agreement are represented by dashed lines.

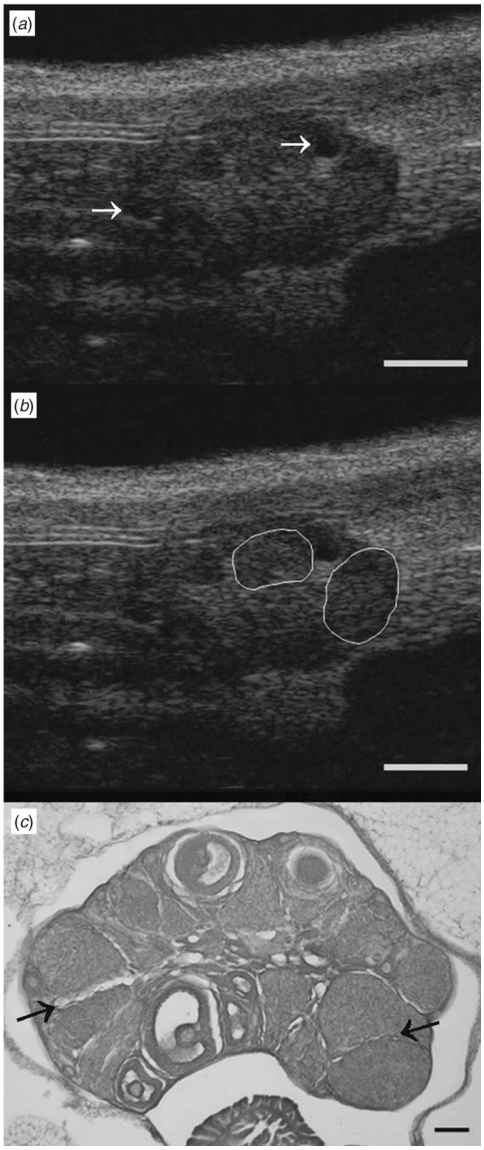

Fig. 3.

Ultrasound biomicroscopy and histological sections of a mouse ovary depicting different-sized corpora lutea. (*a*) UBM images depicting CL ranging from 780 to 970 μm in diameter are (*b*) outlined for clarity. (*a*) Arrows in the UBM image indicate ovarian follicles ranging from 220 to 385 μm in diameter. (*c*) Histology image shows multiple CL ranging in size from 270 to 570 μm. Histology confirmed that CL were not larger than 750 μm. (*c*) Arrows in the histology image indicate interfaces between adjacent CL that were easily visualised by histology. Scale bar: (*a*, *b*) 1000 μm, (*c*) 200 μm.

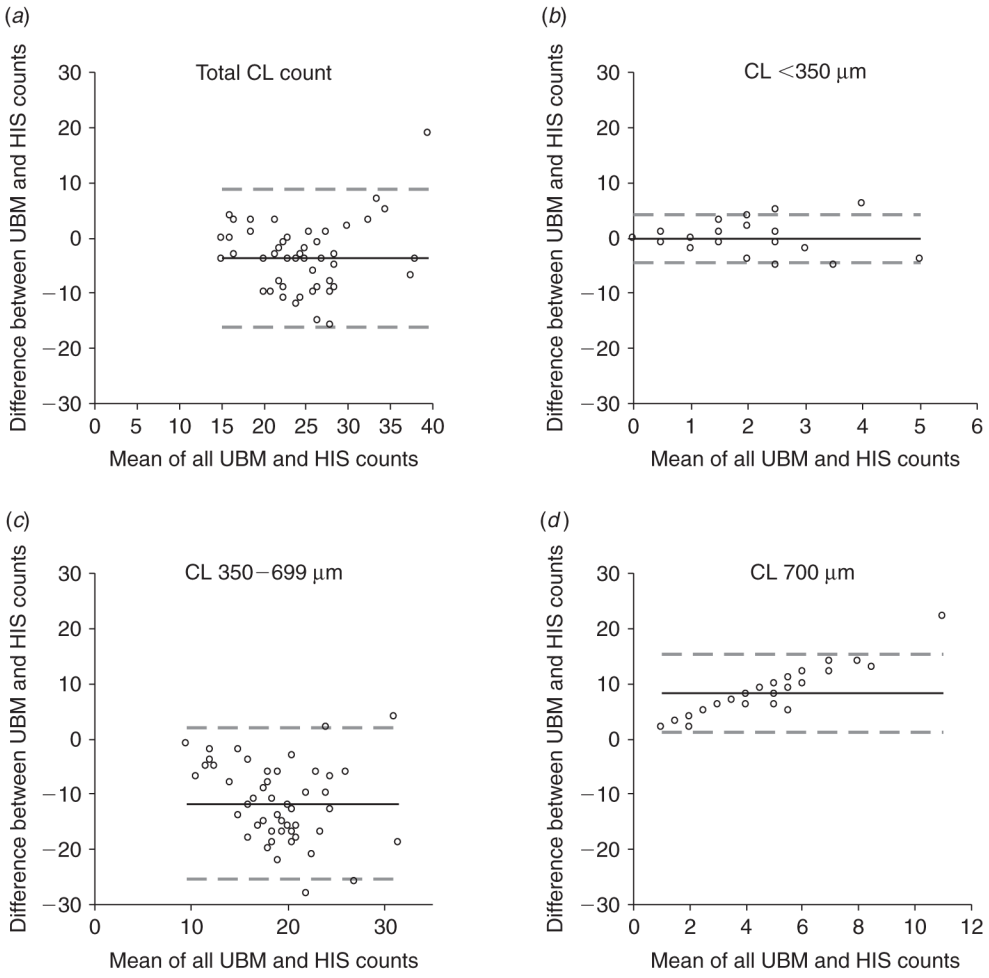

Fig. 4.

Bland-Altman plots for differences in corpora lutea counts made by ultrasound biomicroscopy (UBM) and histology (HIS) for (*a*) the total number of CL, (*b*) CL <350 μm in diameter, (*c*) CL between 350 and 699 μm in diameter and (*d*) CL ≥700 μm in diameter. Difficulty in distinguishing between adjacent CL caused CL 350–699 μm to be underestimated and CL ≥700 μm to be overestimated. Bias is represented by a solid line. Limits of agreement are represented by dashed lines.

Table 1

Bland-Altman agreement statistics for differences in follicle counts made by ultrasound biomicroscopy (UBM) and histology (HIS)

Follicle size	Mean UBM counts	Mean HIS counts	Bias	95% CI for bias	95% Limits of agreement
200–299 μm	3.4	7.4	4.0	−5.3 to −2.7	−12.8 to 4.9
300–399 μm	5.2	6.0	−0.8	−2.0 to 0.3	−8.5 to 6.8
400–499 μm	1.7	0.9	0.8	0.4 to 1.3	−2.4 to 4.1
≥500 μm	0.1	0.1	0.0	–	–
All sizes	10.4	14.4	−4.0	−4.9 to −3.1	−10.5 to 2.5

Table 2

Bland-Altman agreement statistics for differences in corpora lutea counts made by ultrasound biomicroscopy (UBM) and histology (HIS)

CL size	Mean UBM counts	Mean HIS counts	Bias	95% CI for bias	95% Limits of agreement
<350 μm	0.9	1.2	−0.3	−0.9 to 0.4	−4.6 to 4.1
350–699 μm	13.3	25.0	−11.7	−13.7 to −9.7	−25.5 to 2.1
≥700 μm	8.5	0.3	8.2	7.2 to 9.3	1.3 to 15.2
All sizes	22.8	26.6	−3.8	−5.5 to −1.9	−16.2 to 8.7